Shared Autonomous Electric Vehicle Design and Operations under Uncertainties: A Reliability-based Design Optimization Approach

Ungki Lee

Department of Mechanical Engineering, Korea Advanced Institute of Science and Technology,

Daejeon 34141, South Korea

lwk920518@kaist.ac.kr

Namwoo Kang*

Department of Mechanical Systems Engineering, Sookmyung Women's University,

Seoul 04310, South Korea

nwkang@sm.ac.kr

Ikjin Lee*

Department of Mechanical Engineering, Korea Advanced Institute of Science and Technology,

Daejeon 34141, South Korea

ikjin.lee@kaist.ac.kr

* Co-corresponding authors

Abstract

Shared autonomous electric vehicles (SAEVs) are a promising car-sharing service expected to be implemented in the near future. However, existing studies on the optimization of SAEV systems do not consider uncertainties in the SAEV systems, which may interfere with the achievement of the desired performance or objective. From the perspective of the company, an SAEV system should be designed to minimize the total cost while securing the targeted wait time of the customer, but uncertainties in the SAEV system can cause variation in the customer wait time, which can lead to inconveniences to customers and damage to the reputation of the company. Therefore, this study considers the uncertainties in an SAEV system and applies reliability-based design optimization (RBDO) to the design of the SAEV system to minimize the total cost of system design while satisfying the target reliability of the customer wait time. A comparison of the optimization results of various wait time constraints and probabilities of failure provides observations on applying RBDO to the design of an SAEV system. Furthermore, several insights can be obtained through various parametric studies. From this study, it is verified that RBDO can be successfully applied to the design of an SAEV system and a design framework for the SAEV system that can both lower the cost and ensure the reliability of the customer wait time is proposed.

Keywords: Shared autonomous electric vehicle (SAEV), reliability-based design optimization (RBDO), design and operations under uncertainties

1. Introduction

Vehicle electrification is a promising way to reduce fuel consumption and address concerns about environmental pollution and greenhouse gases (GHG) emissions resulting from the use of fossil fuels in transportation systems (Fiori et al., 2016; Tu et al., 2016; Miao et al., 2019). Compared with a conventional vehicle, an electric vehicle (EV) can drive the same distance at approximately half the cost and reduce GHG emissions by 50% (Mak et al., 2013; U.S. Department of Energy report, 2015). Autonomous driving technology is expected to revolutionize transportation systems over the next few decades, providing customers with safe and low-stress transportation solutions (Litman, 2014; Chen et al., 2017), reducing mobility costs (Bösch et al., 2017; Hyland and Mahmassani, 2018), and improving transportation accessibility (Meyer et al., 2017). By integrating EV and autonomous technologies and combining their advantages, an autonomous electric vehicle (AEV) can be proposed, and car-sharing services can be combined with an AEV to offer a more sustainable and marketable car-sharing service (Kang et al., 2016a). Therefore, many operation frameworks and simulation models related to shared

autonomous electric vehicles (SAEVs) have been developed (Chen et al., 2016; Chen and Kockelman, 2016; Loeb et al., 2018; Iacobucci et al., 2018; Farhan and Chen, 2018). Furthermore, many researchers have studied the optimization of the design and operation of SAEV systems. Miao et al. (2019) built a two-stage multi-objective optimization model for an SAEV system and optimized the geographical service area and the allocation of charging infrastructures. Kang et al. (2016a) optimized an SAEV system including vehicle design, fleet assignment, station locations, and service demand, and compared the results with the optimization results of a shared autonomous vehicle system. Liang et al. (2016) maximized the daily profit expected from an electric automated taxi system by deciding service zone locations and whether to accept reservations. Iacobucci et al. (2019) optimized vehicle fleet charging for an SAEV.

However, existing studies on the optimization of an SAEV system focus on the deterministic optimization (DO) problem and do not consider the uncertain factors in the SAEV system, which can have a significant impact on the optimization results of the SAEV system. Various uncertainties such as battery cell characteristics, the initial state-of-charge (SOC) of the battery, real-time traffic, customer's origin and destination, and trip request time can affect the design of an SAEV system. Because of these uncertainties, there may be variations in the objective function of the optimization problem of an SAEV system and the targeted optimum value may not be achieved. In recent times, attempts have been made to solve the optimization problem considering the uncertainties in the system (Youn et al., 2004; Lee et al., 2010; Lee et al., 2011).

Reliability-based design optimization (RBDO) minimizes the objective function of a system and ensures the target reliability of the system by considering the variation of the objective function induced by the uncertainties in the system. In the formulation of RBDO, the target reliability requirements are included in the form of probabilistic constraints and various types of objective functions such as profit maximization, weight minimization, and cost minimization are used (Zou and Mahadevan, 2006). Reliability analysis, an important research topic in RBDO, evaluates the probabilistic constraints considering the uncertainty of the design variables or parameters and quantifies the reliability of the system by predicting the probability of failure (Lee and Jung, 2008). RBDO has been successfully applied in many engineering fields such as mechanical engineering (Choi and Youn, 2002; Youn et al., 2005; Noh et al., 2009; Lee et al., 2013; Zhao et al., 2013; Lim et al., 2015), aerospace engineering (Frangopol and Maute, 2003; Lee et al., 2009; Missoum et al., 2010), composite structures (Qu et al., 2003; Thompson et al., 2006; Luo et al., 2011), civil engineering (Chiti et al., 2016; Nguyen et al., 2013), and traffic engineering (Shin and Lee, 2014, 2015).

Existing DO problems of SAEV systems consider customer wait time as a constraint or a factor affecting the objective function; however, ensuring the reliability of the customer wait time is an important issue as the uncertainties in the system cause a large variation in the customer wait time, which can lead to inconveniences to customers, damage to the reputation of the company, and further deterioration of profitability. Therefore, this study considers the uncertainties in the SAEV system and introduces RBDO to study a system design that minimizes the cost of system design while satisfying the target reliability of the customer wait time. In this study, real road connections of a city are realized through nodes and segments, and simulation reflecting the real-time traffic of each segment is performed. Several observations on applying RBDO to the design of the SAEV system are obtained through a comparison of optimization results using various wait time constraints and target reliabilities. Global sensitivity analysis of uncertainties in the SAEV system is performed using Sobol's method to evaluate the influence of each uncertainty on the SAEV system. In addition, several parametric studies are performed to obtain some insights related to applying RBDO to the design of the SAEV system under different conditions.

The rest of this paper is organized as follows. Section 2 introduces the design framework of an SAEV system including the associated models, real-time traffic reflection, and uncertainties in the SAEV system. Section 3 presents formulations for applying RBDO and DO to the design of the SAEV system. Section 4 compares the results of performing RBDO by changing the wait time constraint and target reliability, and presents insights obtained from parametric studies. Finally, Section 5 summarizes the conclusions of this study and describes its limitations and future research directions.

2. Modeling: SAEV System under Uncertainties

This study extends and modifies the system design framework presented by Kang et al. (2016a) to apply RBDO to the design of an SAEV system successfully for more realistic traffic situations: 1) realizing real road connections using nodes and segments; 2) reflecting real-time traffic of each road; 3) adding the number of chargers in the charging station (CS) design; and 4) setting free floating so that a vehicle moves after service or when not in service. In the design framework of the SAEV system presented in Fig. 1, the fleet operation model, the CS model, and the SAEV design model are integrated and the decision variables, as listed in Table 1, are the fleet size, the number of CSs, the number of chargers in each CS, and the number of battery cells in series and parallel. The fleet operation model reflects real-time traffic in each road section and determines the shortest time path search, SAEV free floating, the charging schedule, and the optimal fleet assignment; the CS model

determines the total number of chargers and the optimal locations of CSs; and the SAEV design model determines the charging time and EV performances such as top speed, acceleration, driving range, and miles per gallon gasoline equivalent (MPGe). The output of the framework is the total cost and customer wait time, which are used as the objective function and probabilistic constraint in the RBDO formulation, respectively. In this study, we assume that the SAEV system operator owns the CSs and can decide about the CS design, and appropriate fleet assignment can be performed by centrally managing all SAEV statuses, locations, and trip requests in real time.

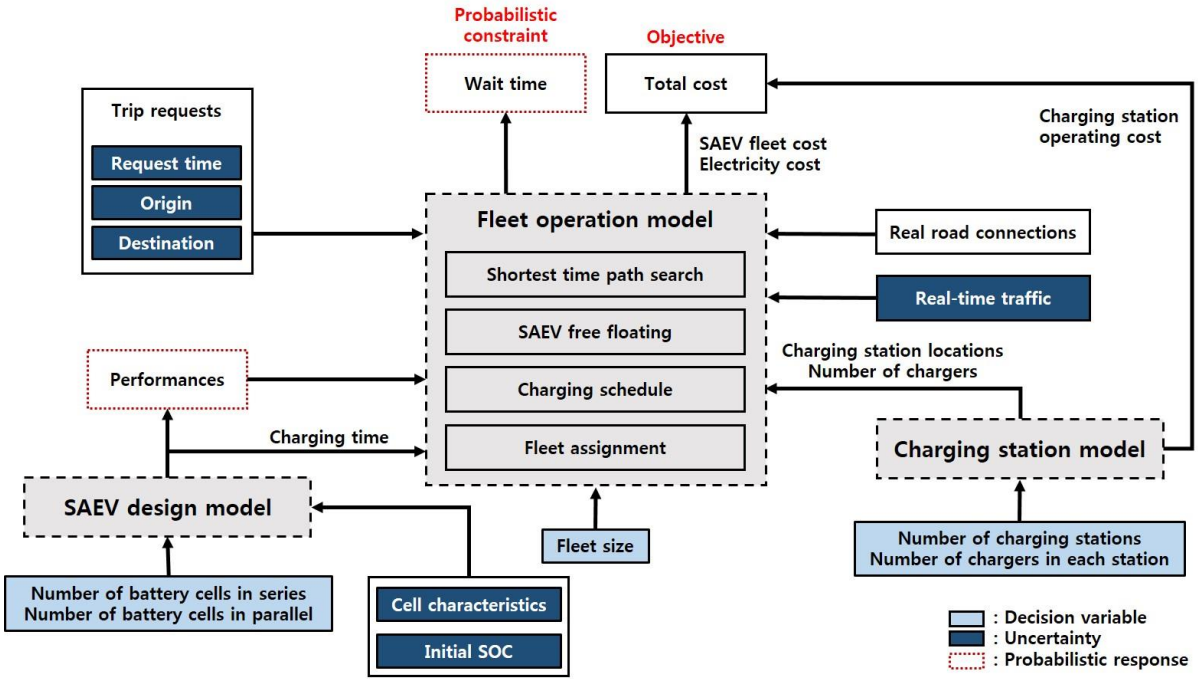

Fig. 1 Design framework of the SAEV system

Table 1 Decision variables and their bounds for SAEV design

Design variable	Lower bound	Upper bound
Fleet size	5	100
Number of CSs	1	10
Number of chargers in each CS	1	10
Number of battery cells in series	80	250
Number of battery cells in parallel	1	4

2.1 Fleet operation model

Operation and scheduling problems are the main factors in transportation system design (Marwaha and

Kokkolaras, 2015). In the fleet operation model, fleets are appropriately operated and assigned according to trip requests and the given decision variables, and the customer wait time and SAEV fleet cost are provided as outputs. In this study, we assume that the SAEV replaces some part of the traditional transportation and 100 customers use the SAEV service per day. Further parametric studies may provide results and trends when the number of trip requests per day changes. As shown in Fig. 2, the main area of Daejeon, Korea is used as the test bed of this study. The crossing points of each road are set as nodes, and the segments are connected to each other to represent real roads. The test bed has a total of 128 nodes and 199 segments. By representing the roads as sets of nodes and segments, determining the shortest path or the shortest time path becomes easier and reflecting the traffic of each road section becomes possible. The optimal CS locations in the figure will be covered in Section 2.2.

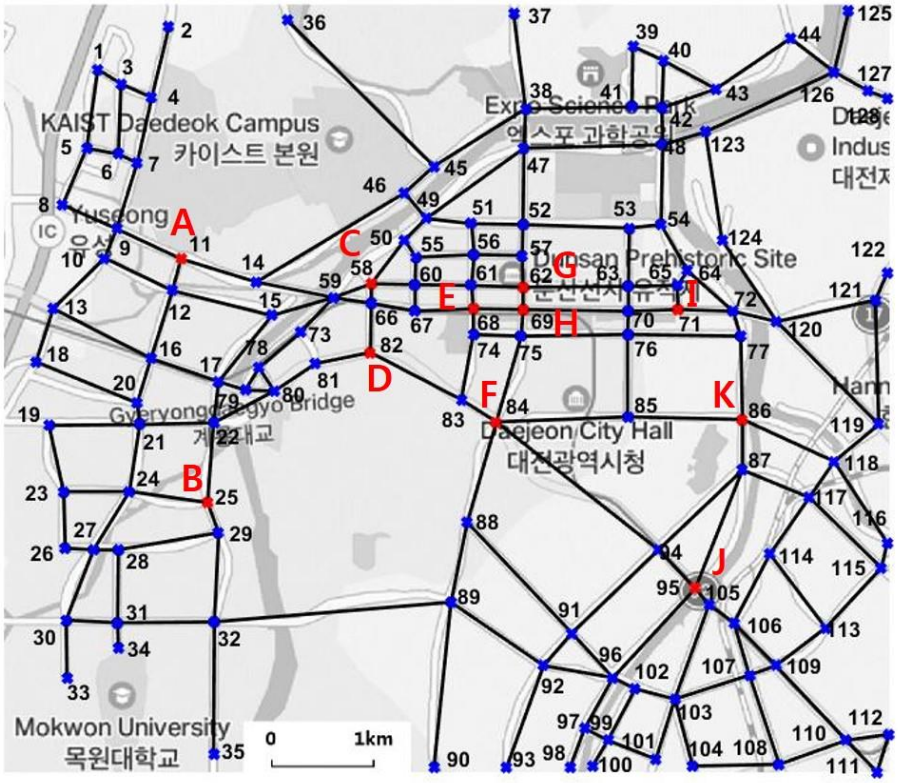

Fig. 2 Schematic representation of the road connections and the candidates of CS locations in Daejeon

In the operation of the SAEV system, there are three states of the fleet: 1) the idle state where the vehicle is not in service and can come to the customer immediately when a request occurs; 2) the in-service where the vehicle is occupied and can come to the customer after service; and 3) the charging state where the vehicle is charging and can come to the customer after charging. The flowchart of the SAEV fleet operation is shown in Fig. 3 and one simulation runs for 24 h. The initial locations of the vehicle on the first day are set randomly, and the

last vehicle locations on the previous day are used as the initial locations for the simulation of the next day. In the idle state, the fleet is free floating and moves randomly to another node. During free floating, the SOC of the battery capacity is continuously monitored by a central operating system and the vehicle goes to the CS when the SOC of the vehicle battery reaches its lower bound. If all the chargers in the CSs are occupied, the charger with the least wait time is assigned, whereas the closest charger is assigned if there are empty chargers. The central operating system monitors the time the vehicle starts and ends charging at the CS and adjusts the charging schedule. When a trip is requested, the vehicle with feasible SOC, i.e., the one having sufficient SOC to go from the current location to the customer and go to the nearest CS after service, is included among the candidate vehicles that can go to the service. Among the candidate vehicles, the vehicle that minimizes the customer's wait time is then selected. After the service is finished, the battery SOC is checked and the vehicle starts free floating.

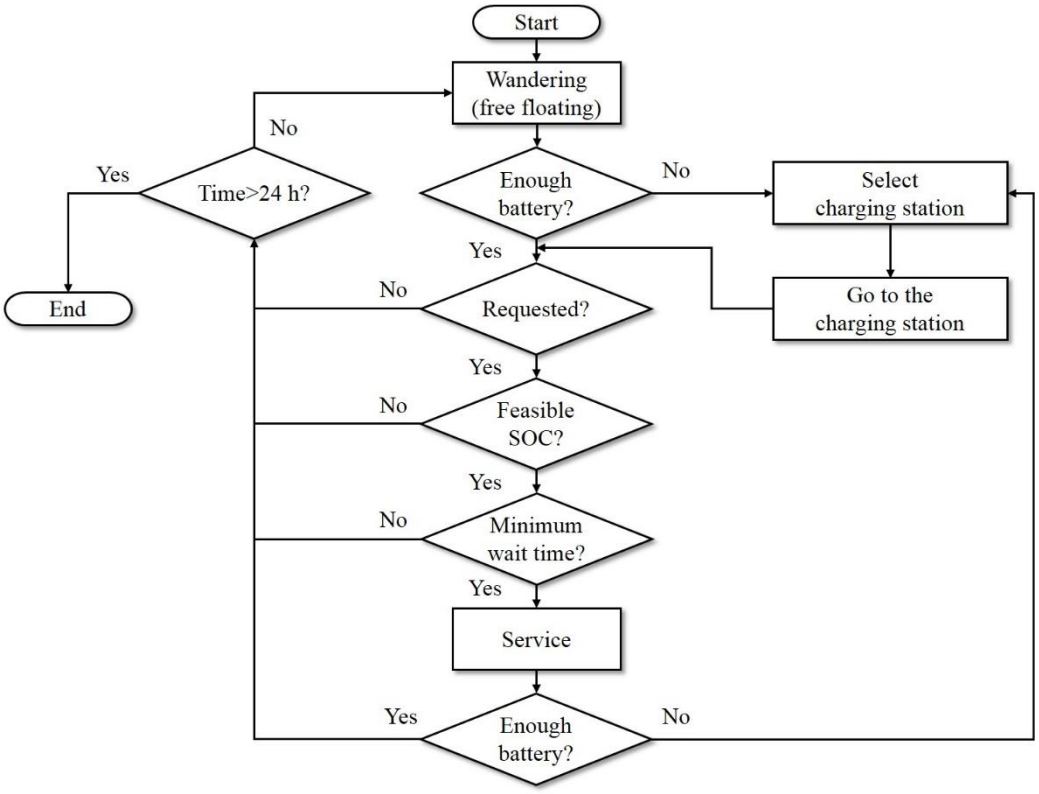

Fig. 3 Flowchart of the fleet operation of the SAEV

To obtain the shortest path from the vehicle's current location to the customer, from the customer's origin to the destination, or from the vehicle's current location to the CS, the shortest path algorithm proposed by Dijkstra

(1959) is used. After determining the shortest path, the time required for the path can be obtained once the speed of the vehicle is provided. If the speed of the vehicle in each path is different owing to the traffic, the shortest time path can be obtained. The application of traffic to the Dijkstra algorithm will be explained in Section 2.4.

The fleet operations of the SAEV are as follows:

1. The trip request time is generated based on the distribution of the floating population of Daejeon per time provided by the Korean government (Daejeon Metropolitan City website, 2019).
2. When a customer submits his or her origin and destination via a smartphone app, the central operating system combines it with the request time into a single completed trip request and assigns the appropriate SAEV.
3. The origin and destination of the customer can be anywhere on the map: the SAEV moves to the node nearest to the requested point and moves out of the segment to reach the requested point.
4. The assigned SAEV goes to the customer's origin along the shortest time path and also takes the customer to the destination along the shortest time path.
5. When real-time traffic is not considered, the average speed of the SAEV is assumed to be 35.4 km/h, which is the daily average speed of taxis surveyed by the Korea Ministry of Land, Infrastructure, and Transport (Korea Ministry of Land, Infrastructure and Transport Website, 2011).

2.2 CS model

The CS model determines the total number of chargers and the optimal CS locations. Similar to the method proposed by Kang et al. (2016b), the *p*-median model is used to determine the candidates of CS locations in Daejeon (Tansel et al., 1983). The candidates of CS locations are selected to minimize the path distance between any node and its closest CS. As presented in Fig. 1, the candidates of CS locations are pre-determined before the simulation, and as the number of CSs, which is one of the decision variables, is determined, the locations of the CSs are determined as shown in Table 2. The total number of chargers, which is determined by the number of CSs and the number of chargers in each station, is related to the capacity of the CSs and affects the customer wait time by determining the CS wait time, which is the duration for which the SAEV should wait on the CS when all the chargers of CSs are occupied.

The operating cost of the CS includes the installment and maintenance costs, which are assumed to be \$22,626 and \$5,000, respectively, for each charger (Kang et al., 2016a; EERE website, 2016). The average

charging fee of an EV in Korea, i.e., 9.1 cents/kWh, is used as the electricity cost (Electric Vehicle Charging Information System website, 2019).

Table 2 Candidates of CS locations in Daejeon (A to K)

Number of CSs	Candidates of CS locations
1	E
2	D,K
3	C,H,J
4	C,G,I,J
5	B,C,G,I,J
6	B,C,F,G,I,J
7	A,B,C,F,G,I,J
8	A,B,C,E,F,G,I,J
9	A,B,C,D,F,G,I,J,K
10	A,B,C,D,E,F,G,I,J,K

2.3 SAEV design model

In the SAEV design model, the EV simulation model presented by Lee et al. (2019) is used to determine vehicle performances such as range, top speed, acceleration, and MPGe based on the design of a powertrain. As only the range of vehicle performances affects the customer wait time and it is linearly related to the gear ratio (Zhou et al., 2013), the gear ratio is assumed to be 8.2 for Nissan Leaf (EV Specifications website, 2019). The Neural Networks package of MATLAB is used to build the metamodel of the SAEV design model. The performances, which are the outputs of the SAEV design model, are used as the inputs of the fleet operation model and are also used as the minimum performance constraints for the vehicle to drive in the real world: the top speed should be faster than 120 km/h, acceleration from 0 to 100 km/h should be shorter than 20 s, and the range should be more than 60 km. In this study, a direct-current fast charger capable of charging a 24 kWh battery within 30 min is assumed and the charging time is estimated depending on the battery capacity.

Based on the SAEV design model, the cost of each SAEV, which consists of the sum of the following costs, can be estimated: the cost of a lithium-ion battery is assumed to be $236/kWh (The Mack Institute website, 2017); the cost of an 80 kW permanent magnet synchronous motor is assumed to be $1,665 (Simpson, 2006); the cost of an autonomous module is assumed to be $10,000 (Kang et al., 2016a); and other costs for the vehicle are assumed to be fixed at $6,000.

2.4 Real-time traffic

The shortest path and the shortest time path differ depending on the real-time traffic conditions. Therefore,

it is important to consider the real-time traffic in the design of the SAEV system as the optimal fleet size, the number of CSs and chargers, and the battery capacity can vary owing to the changed path. To reflect the real-time traffic of Daejeon, the NAVER map (NAVER website, 2019), which provides the real-time average speed information of Korean roads, is used to determine the average speed of each road section and the average speed of road sections over every hour is presented in Table 3. The table shows a significant decrease in the average speed during rush hour and a smooth traffic flow at dawn, which are similar to the real-time traffic conditions in a typical city.

Table 3 Average speed of road sections over time

Time	0–20 km/h	20–40 km/h	40–60 km/h	60–80 km/h	Average speed (km/h)
0:00–1:00	0.00%	0.00%	97.47%	2.53%	47.6
1:00–2:00	0.00%	0.00%	97.98%	2.02%	47.7
2:00–3:00	0.00%	0.00%	98.48%	1.52%	47.5
3:00–4:00	0.00%	0.00%	97.47%	2.53%	47.8
4:00–5:00	0.00%	0.00%	98.48%	1.52%	47.8
5:00–6:00	0.00%	0.00%	98.99%	1.01%	47.3
6:00–7:00	66.67%	30.81%	2.53%	0.00%	17.6
7:00–8:00	59.09%	37.88%	3.03%	0.00%	19.1
8:00–9:00	57.07%	37.88%	5.05%	0.00%	20.5
9:00–10:00	50.51%	45.96%	3.54%	0.00%	21.8
10:00–11:00	41.41%	53.54%	5.05%	0.00%	23.3
11:00–12:00	38.89%	55.05%	6.06%	0.00%	24.3
12:00–13:00	33.84%	57.58%	7.58%	1.01%	25.6
13:00–14:00	27.27%	63.64%	8.08%	1.01%	26.7
14:00–15:00	27.78%	61.62%	9.09%	1.52%	27.7
15:00–16:00	32.32%	59.60%	7.58%	0.51%	25.4
16:00–17:00	44.95%	50.00%	5.05%	0.00%	22.4
17:00–18:00	58.59%	36.87%	4.55%	0.00%	19.8
18:00–19:00	27.78%	62.12%	9.60%	0.51%	26.7
19:00–20:00	11.62%	26.77%	59.09%	2.53%	39.7
20:00–21:00	2.02%	7.58%	88.89%	1.52%	45.4
21:00–22:00	0.00%	2.02%	95.96%	2.02%	47.1
22:00–23:00	0.00%	1.01%	95.96%	3.03%	47.7
23:00–24:00	0.00%	0.00%	97.47%	2.53%	47.7

The real-time traffic of each road section is applied to the Dijkstra algorithm by recognizing the length of each section differently according to the average speed of each section: if the average speed of the road section is higher than the average speed of the SAEV, which is assumed to be 35.4 km/h, the Dijkstra algorithm considers the length of the road section to be shorter than the actual length and then derives the shortest path. Fig. 4 shows an example of the shortest time path from node 1 to node 109 according to time obtained by considering real-time traffic and compares it with the path obtained when real-time traffic is not considered. The color bar on the right side of the figure indicates the average speed of the road section, in units of kilometer per hour, and the average

speed is 35.4 km/h when real-time traffic is not considered. In each case, the travel distance and the time required for the shortest time path are as follows: (a) 9.9 km and 13.9 min; (b) 13.0 km and 43.7 min; (c) 10.4 km and 31.6 min; and (d) 9.9 km and 16.8 min, respectively. The figure shows that the path that is not the shortest distance can be selected to avoid heavy traffic and the shortest time path varies from hour to hour.

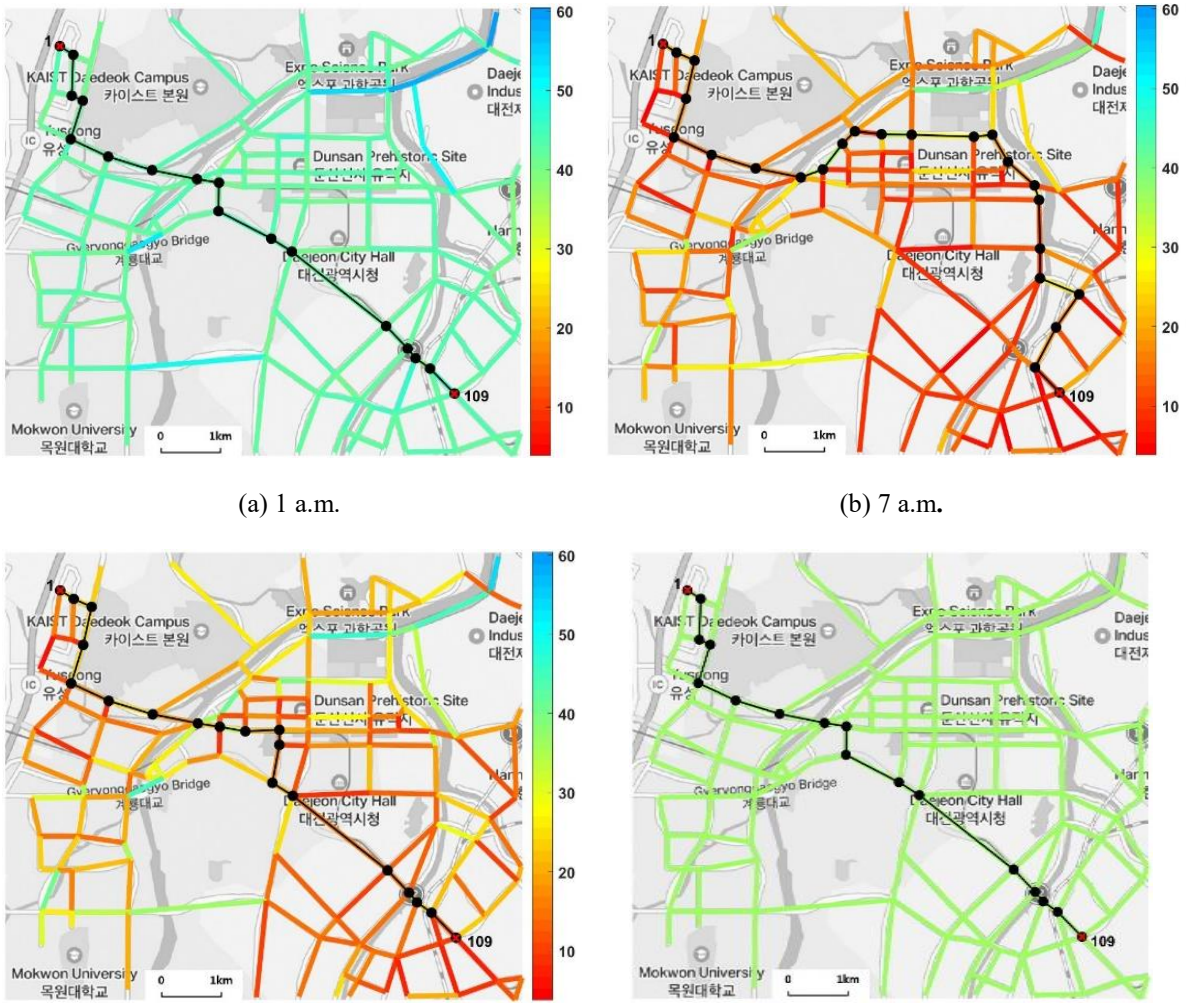

(a) 1 a.m.

(b) 7 a.m.

(c) 10 a.m.

(d) Real-time traffic is not considered

Fig. 4 An example of the shortest time path from node 1 to node 109

2.5 Uncertainties in the SAEV system

In the SAEV system, there are uncertainties in the traffic and trip requests in addition to the engineering uncertainties related to the battery or the initial SOC, resulting in a variation in the customer wait time and a decrease in the reliability. The properties of the aforementioned uncertainties that may exist in the SAEV system are presented in Table 4. A Li-ion battery is considered one of the best energy sources of EVs; however, variations

in the battery cell characteristics exist owing to uncertainties in the material and the physical property resulting from the manufacturing process (Jing et al., 2014; Tong et al., 2015). Furthermore, uncertainties in cell properties such as solid particle size or porosity affect the deviations in cell characteristics (Hadigol et al., 2015). This study uses the distributions of cell characteristics obtained from the statistical and electrochemical analyses of Li-ion battery cells presented by Dubarry et al. (2010). At the start of the simulation, the initial SOC of the SAEV also has a variation, and 80% SOC is usually assumed (Kang et al., 2016a). This study assumes that the initial SOC follows a normal distribution with the mean and coefficient of variation (COV) of 80% and 5.0%, respectively.

Table 4 Properties of uncertainties in the SAEV system

	Mean	COV*	Distribution type
Cell capacity	33.1 Ah	1.5%	Normal
Cell voltage	3.8 V	0.5%	Normal
Cell weight	0.7864 kg	2.0%	Normal
Initial SOC	80%	5.0%	Normal
Traffic	Data**	5.0%	Normal
Origin & Destination	Randomly generated considering traffic		
Request time	Drawn randomly from the distribution of person request per day		

* Coefficient of variation
** Data collected for each road section

In this study, real-time traffic is reflected based on the average speed data of each road section. As the average speed of each road section is not deterministic, the uncertainty of traffic should also be considered. Based on the obtained real-time traffic data, the traffic in each road section is assumed to follow a normal distribution whose mean is the average speed of each road section and whose COV is 5.0%.

The uncertain factors associated with trip requests are the origin and destination of the customer and the request time. In this study, assuming that there will be many trip requests near heavy traffic, the origins and destinations of customers are randomly generated by considering the traffic in each road section in every hour. The trip request time of each customer is randomly sampled from the distribution of daily person trips in Daejeon indicated in Daejeon Metropolitan City website (2019). The generated origin, destination, and request time constitute a trip request containing uncertainty, which should be considered when operating the SAEV.

3. Optimization: RBDO Approach

Many existing SAEV system optimization problems focus on DO without considering system uncertainties; consequently, the derived design is not optimal for the actual operation of the SAEV and can decrease the

reliability of the output owing to the occurrence of variation. This section presents RBDO for the design of the SAEV system, and compares it with DO formulations.

3.1 RBDO formulation

The problem of applying RBDO to the design of the SAEV system can be formulated as

$$
\begin{aligned}
\text{find} \quad & \mathbf{X}=\left[\mathbf{X}_{batt}^{\mathrm{T}}, N_{\mathrm{SAEV}}, N_{\mathrm{CS}}, N_{\mathrm{charger}}\right] \\
\min_{\mathbf{X}} \quad & \mathrm{Cost}(\mathbf{X}) \\
\text{subject to} \quad & \mathbf{lb} \le \mathbf{X} \le \mathbf{ub} \\
& \mathbf{g}\left(\mathbf{X}_{batt}\right) \le 0 \\
& P\left[G\left(\mathbf{W}\right) > 0\right] \le P_F^{\mathrm{Target}} \\
\text{where} \quad & \mathbf{X}_{batt}=\left[N_{\mathrm{S}}, N_{\mathrm{P}}\right]^{\mathrm{T}} \\
& P_F^{\mathrm{Target}} = 1-R \\
& \mathbf{P}=\left[P_{\mathrm{range}}, P_{\mathrm{speed}}, P_{\mathrm{accel}}, P_{\mathrm{MPGe}}\right] \\
& \mathbf{RP}=\left[\mathbf{RP}_{\mathrm{engineering}}, \mathbf{RP}_{\mathrm{traffic}}, \mathbf{RP}_{\mathrm{customer}}\right] \\
& \left[\mathbf{L}_{\mathrm{CS}}, C_{\mathrm{CS}}\right] = f_{\mathrm{CS}}\left(N_{\mathrm{CS}}, N_{\mathrm{charger}}\right) \\
& \left[\mathbf{P}, P_{\mathrm{charging}}\right] = f_{\mathrm{SAEV}}\left(\mathbf{X}_{batt}\right) \\
& \left[\mathbf{W}, C_{\mathrm{SAEV}}\right] = f_{\mathrm{operation}}\left(N_{\mathrm{SAEV}}, \mathbf{L}_{\mathrm{CS}}, N_{\mathrm{charger}}, P_{\mathrm{range}}, P_{\mathrm{charging}}, \mathbf{RP}\right)
\end{aligned}
\quad , \tag{1}
$$

where the objective is to minimize the total cost consisting of the SAEV fleet cost, electricity cost, and CS operating cost; $\mathbf{X}$ is a deterministic decision variable vector; $\mathbf{X}_{batt}$ indicates the battery design variable vector; N_{SAEV}, N_{CS}, and N_{charger} are the SAEV fleet size, the number of CSs, and the number of chargers, respectively; **lb**, **ub**, **g**, and G represent the lower bound, upper bound, minimum performance constraint, and probabilistic constraint related to the customer wait time distribution, respectively; $P[\cdot]$ is the probability measure; P_F^{Target} indicates the target probability of failure; R is the target reliability; $\mathbf{P}$ represents the performance vector; $\mathbf{RP}$ denotes the random parameter matrix of the fleet operation model; $\mathbf{L}_{\mathrm{CS}}$ is the vector of CS locations; C_{CS} is the CS operating cost including the installment and maintenance costs of CSs; $\mathbf{W}$ is the customer wait time distribution; C_{SAEV} is the cost of the SAEV fleet; P_{charging} indicates the charging time of the SAEV; and f_{CS}, f_{SAEV}, and $f_{\mathrm{operation}}$ indicate the CS model, SAEV design model, and fleet operation model, respectively.

To evaluate the probabilistic constraint in Eq. (1), reliability analysis is performed to obtain the probability of failure, which is calculated as

$$
P_F = P\left[\mathbf{X} \in \Omega_F\right] = P\left[G\left(\mathbf{X}\right) > 0\right] = \int_{\Omega_F} f_{\mathbf{X}}(\mathbf{x})\mathrm{d}\mathbf{x} \,, \tag{2}
$$

where Ω_F is the failure set defined as $\{\mathbf{x}: G(\mathbf{X}) > 0\}$ and $f_{\mathbf{X}}(\mathbf{x})$ indicates the joint probability density function of $\mathbf{X}$.

In this study, reliability analysis is performed using Monte Carlo simulation as it facilitates an accurate analysis with a large number of simulations when the simulation is computationally efficient.

When the wait time constraint and target reliability are provided, a probabilistic constraint can be established, and the probability of failure can be used to determine whether the system fails or not. For example, assuming that the target reliability is 95% and the failure is defined as a case where the customer wait time is greater than 10 min, the wait time constraint becomes 10 min and the amount of customer wait time that exceeds 10 min should be less than 5% of the total distribution of the customer wait time to satisfy the target reliability. Various combinations of wait time constraint and target reliability are examined to investigate their influence and importance: the wait time constraints are 6, 8, 10, and 12 min and the target reliabilities are 90% and 95%.

3.2 DO formulation

This study also compares the results of applying DO to the results of RBDO to determine the importance of applying RBDO. The DO of the design of the SAEV system is formulated as follows:

$$
\begin{aligned}
\text{find} \quad & \mathbf{X}=\left[\mathbf{X}_{batt}^{\mathrm{T}}, N_{\mathrm{SAEV}}, N_{\mathrm{CS}}, N_{\mathrm{charger}}\right] \\
\text{subject to} \quad & \mathbf{lb} \le \mathbf{X} \le \mathbf{ub} \\
& g_{\mathrm{SAEV}}(W) \le 0 \\
\text{where} \quad & \mathbf{X}_{batt}=\left[N_{\mathrm{S}}, N_{\mathrm{P}}\right]^{\mathrm{T}} \\
& \mathbf{P}=\left[P_{\mathrm{range}}, P_{\mathrm{speed}}, P_{\mathrm{accel}}, P_{\mathrm{MPGe}}\right] \\
& \mathbf{RP}=\left[\mathbf{RP}_{\mathrm{engineering}}, \mathbf{RP}_{\mathrm{traffic}}, \mathbf{RP}_{\mathrm{customer}}\right] \\
& \left[\mathbf{L}_{\mathrm{CS}}, C_{\mathrm{CS}}\right]=f_{\mathrm{CS}}\left(N_{\mathrm{CS}}, N_{\mathrm{charger}}\right) \\
& \left[\mathbf{P}, P_{\mathrm{charging}}\right]=f_{\mathrm{SAEV}}\left(\mathbf{X}_{batt}\right) \\
& \left[W, C_{\mathrm{SAEV}}\right]=f_{\mathrm{operation}}\left(N_{\mathrm{SAEV}}, \mathbf{L}_{\mathrm{CS}}, N_{\mathrm{charger}}, P_{\mathrm{range}}, P_{\mathrm{charging}}, \mathbf{RP}\right)
\end{aligned}
\quad , \qquad (3)
$$

where the objective function is the same as that of RBDO, g_{SAEV} is a deterministic constraint, and W indicates the mean customer wait time. In the deterministic constraint of the DO, the mean customer wait time W should be less than the time of the given wait time constraint.

4. Results and Discussion

This section presents the results of applying RBDO to the design of the SAEV system using various wait time constraints and target reliabilities, and also compares the results with the DO results. The wait time constraints of DO and RBDO are 6, 8, 10, and 12 min and the target reliabilities are 90% and 95% for RBDO, as explained in Section 3.2. We use the genetic algorithm for global search and sequential quadratic programming

for local search to solve the optimization problems in Eq. (1) and Eq. (3). Though the computation time varies depending on the fleet size of the fleet operation system, one round of optimization took 22 h on average using a standard desktop (Intel i7 6900 CPU @ 128.0 GB RAM and 3.20 GHz).

4.1 Optimization results and comparison

Tables 5–8 summarize the optimal designs and outcomes of using DO and RBDO according to the wait time constraint. In RBDO, the target reliabilities of 90% and 95% correspond to the target probabilities of failure of 10% and 5%, respectively. The probability of failure in the RBDO design satisfies the target probability of failure and shows that RBDO is successfully applied to the design of the SAEV system. On the contrary, the reliability of the customer wait time in the DO design is relatively low, which can lead to inconvenience to passengers and a decline in the profit of the SAEV company owing to the damage to its reputation. If the time of the wait time constraint of the DO design is 8 min and 12 min, the engineering constraint is active as the range, top speed, and 0 to 100 km/h violate the engineering constraints if the number of battery cells in series is less than 77. Therefore, the probabilistic constraint is inactive, and therefore, the probability of failure becomes relatively low.

Table 5 Optimal designs and outcomes obtained using DO and RBDO (wait time constraint of 6 min)

		DO design	RBDO design	
			P_F^{Target}=10%	P_F^{Target}=5%
Decision variables	Fleet size	11	35	52
	Number of CSs	2	5	7
	Location of CSs	D,K	B,C,G,I,J	A,B,C,F,G,I,J
	Number of chargers	1	1	1
	Number of battery cells in series	120	125	136
	Number of battery cells in parallel	1	1	1
Vehicle spec	Acceleration (0–100)	9.1 s	8.9 s	8.6 s
	Range	100.0 km	104.4 km	112.8 km
	Top speed	154.2 km/h	155.4 km/h	157.6 km/h
	MPGe	139.3	139.2	138.7
	Battery capacity	15.1 kWh	15.7 kWh	17.1 kWh
Cost	Total cost	$289,852	$889,098	$1,325,862
	Fleet cost	$233,498	$748,143	$1,128,506
	CS installment cost	$45,252	$113,130	$158,382
	CS maintenance cost	$11,000	$27,500	$38,500
	Electricity cost per day	$102	$325	$474
Fleet operating	Charging time	18.1 min	18.9 min	20.7 min
	Fleet service distance	6,575 km	20,961 km	30,407 km

	per day			
Customer wait time	Mean	6.0 min	3.3 min	2.7 min
	(Std)	(3.8 min)	(2.2 min)	(1.8 min)
Probability of failure		41.762%	10.027%	4.951%

Table 6 Optimal designs and outcomes obtained using DO and RBDO (wait time constraint of 8 min)

		DO design	RBDO design	
			P_F^{Target}=10%	P_F^{Target}=5%
Decision variables	Fleet size	8	21	32
	Number of CSs	1	2	4
	Location of CSs	E	D,K	C,G,I,J
	Number of chargers	1	1	1
	Number of battery cells in series	77	127	118
	Number of battery cells in parallel	1	1	1
Vehicle spec	Acceleration (0–100)	19.2 s	8.8 s	9.2 s
	Range	63.2 km	105.7 km	98.4 km
	Top speed	120.0 km/h	155.8 km/h	153.7 km/h
	MPGe	140.8	139.1	139.4
	Battery capacity	9.7 kWh	16.0 kWh	14.8 kWh
Cost	Total cost	$187,802	$506,554	$790,157
	Fleet cost	$159,605	$450,132	$677,367
	CS installment cost	$22,626	$45,252	$90,504
	CS maintenance cost	$5,500	$11,000	$22,000
	Electricity cost per day	$70	$169	$285
Fleet operating	Charging time	10.3 min	19.2 min	17.7 min
	Fleet service distance per day	4,450 km	10,893 km	18,404 km
Customer wait time	Mean	7.7 min	4.4 min	3.5 min
	(Std)	(5.1 min)	(2.8 min)	(2.4 min)
Probability of failure		39.202%	10.044%	5.0438%

Table 7 Optimal designs and outcomes obtained using DO and RBDO (wait time constraint of 10 min)

		DO design	RBDO design	
			P_F^{Target}=10%	P_F^{Target}=5%
Decision variables	Fleet size	6	13	20
	Number of CSs	1	2	2
	Location of CSs	E	D,K	D,K
	Number of chargers	1	1	1
	Number of battery cells in series	111	150	96
	Number of battery cells in parallel	1	1	1
Vehicle spec	Acceleration (0–100)	9.5 s	8.3 s	11.0 s

	Range	92.5 km	124.0 km	80.1 km
	Top speed	151.8 km/h	160.0 km/h	145.7 km/h
	MPGe	139.6	138.2	140.2
	Battery capacity	14.0 kWh	18.9 kWh	12.1 kWh
Cost	Total cost	$153,940	$343,900	$466,709
	Fleet cost	$125,760	$287,529	$410,293
	CS installment cost	$22,626	$45,252	$45,252
	CS maintenance cost	$5,500	$11,000	$11,000
	Electricity cost per day	$54	$119	$163
Fleet operating	Charging time	16.6 min	23.1 min	13.8 min
	Fleet service distance per day	3,485 km	7,593 km	10,519 km
Customer wait time	Mean	10.0 min	5.5 min	4.5 min
	(Std)	(7.2 min)	(3.5 min)	(2.9 min)
Probability of failure		40.214%	9.974%	4.945%

Table 8 Optimal designs and outcomes obtained using DO and RBDO (wait time constraint of 12 min)

		DO design	RBDO design	
			P_F^{Target}=10%	P_F^{Target}=5%
Decision variables	Fleet size	6	11	13
	Number of CSs	1	1	2
	Location of CSs	E	E	D,K
	Number of chargers	1	1	1
	Number of battery cells in series	77	80	117
	Number of battery cells in parallel	1	1	1
Vehicle spec	Acceleration (0–100)	19.2 s	16.9 s	9.2 s
	Range	63.3 km	65.9 km	97.4 km
	Top speed	120.0 km/h	126.7 km/h	153.5 km/h
	MPGe	140.8	140.7	139.4
	Battery capacity	9.7 kWh	10.1 kWh	14.7 kWh
Cost	Total cost	$147,885	$248,648	$331,165
	Fleet cost	$119,704	$220,437	$274,794
	CS installment cost	$22,626	$22,626	$45,252
	CS maintenance cost	$5,500	$5,500	$11,000
	Electricity cost per day	$55	$85	$119
Fleet operating	Charging time	10.3 min	10.8 min	17.5 min
	Fleet service distance per day	3,470 km	5,445 km	7,661 km
Customer wait time	Mean	10.4 min	6.4 min	5.4 min
	(Std)	(7.7 min)	(4.2 min)	(3.5 min)
Probability of failure		31.528%	10.007%	5.033%

4.2 Observations and discussion

The following observations can be obtained from the optimal designs and outcomes:

1) *The total cost of the SAEV system that satisfies the target reliability increases significantly as the target*

reliability of the RBDO design increases. The comparison of the total costs of the DO and RBDO designs according to the wait time constraint is shown in Fig. 5. In both DO and RBDO designs, the total cost increases as the wait time constraint decreases. This observation is expected as the SAEV system must be designed conservatively to reduce the wait time of the customers as the wait time constraint decreases. However, the increase rate of the total cost of the RBDO design (56.53%) is greater than that of the DO design (26.81%), and as the target reliability of the RBDO design increases, the increase rate of the total cost tends to increase (from 53.71% to 59.34%). This indicates that lowering the wait time constraint becomes more difficult as the target reliability increases since the SAEV system with high target reliability already pursues high-cost design.

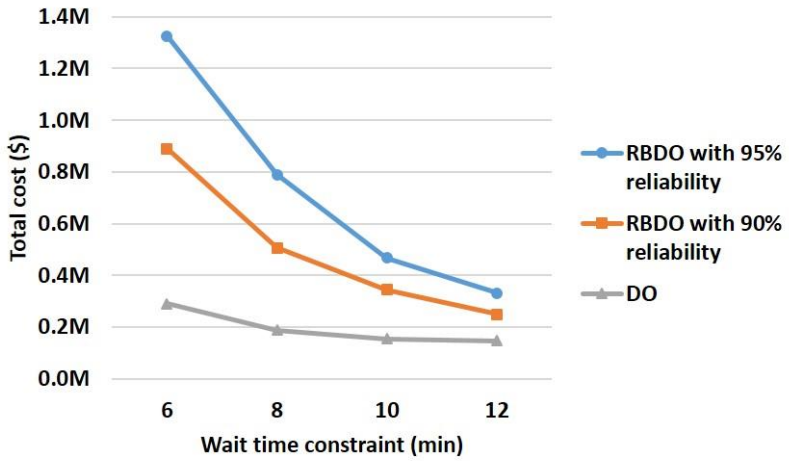

Fig. 5 Comparison of the total costs of the DO and RBDO designs

2) *In both DO and RBDO designs, the fleet size tends to increase as the wait time constraint decreases, and a CS design where chargers are distributed over a large area is preferred.* Fig. 6 presents the comparison of the fleet sizes and battery capacities of the DO and RBDO designs according to the wait time constraint. The increase in fleet size can be regarded as a critical reason for the increase in the total cost. The comparison of fleet sizes and CS designs is shown in Table 9. The number of CSs tends to increase to accommodate the increased fleet size. The number of CSs tends to increase preferentially than the number of chargers in each CS, which shows that the CS design with chargers spread over a larger area can accommodate the SAEVs more efficiently. Similarly, as the target reliability increases, the fleet size tends to increase initially, and the number of CSs tends to increase to accommodate the increased fleet

size. This can be observed for the wait time constraints of 10 min and 12 min.

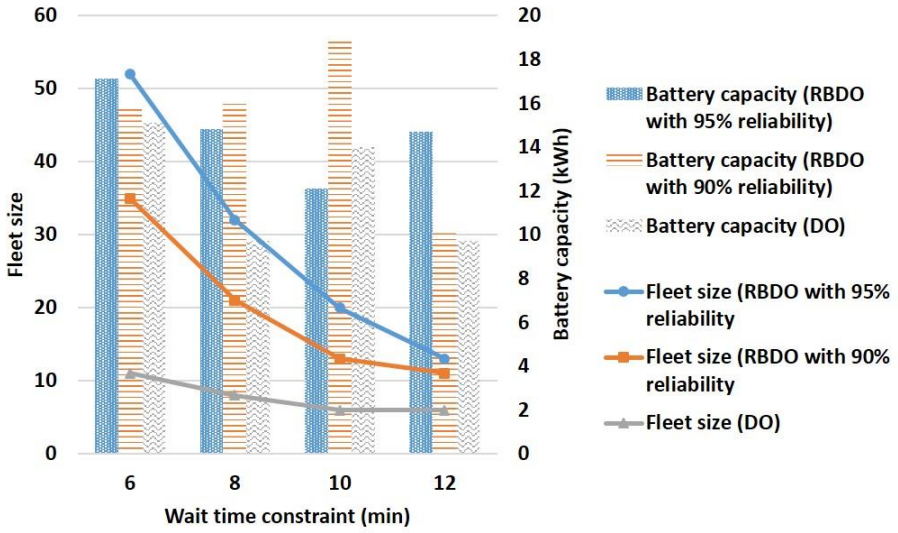

Fig. 6 Comparison of the fleet sizes and battery capacities of the DO and RBDO designs

Table 9 Comparison of fleet sizes and CS designs

Wait time constraint (min)	DO design			RBDO design					
				P_F^{Target}=10%			P_F^{Target}=5%		
	Fleet size	Number of CSs	Number of chargers in each CS	Fleet size	Number of CSs	Number of chargers in each CS	Fleet size	Number of CSs	Number of chargers in each CS
6	11	2	1	35	5	1	52	7	1
8	8	1	1	21	2	1	32	4	1
10	6	1	1	13	2	1	20	2	1
12	6	1	1	11	1	1	13	2	1

3) *There is a tradeoff relationship between the battery capacity and fleet size, and the battery capacity is optimized by considering the cost in addition to the range, CS wait time, and fleet size, which affect the fleet operation.* The battery capacity affects the charging frequency and the number of SAEVs that can

reach the customer. Furthermore, the CS wait time associated with the customer wait time is affected as the battery capacity determines the charging time. These relationships between the battery capacity and fleet operation depend on the fleet size. As the battery capacity determines the battery cost, which affects the fleet cost, the battery capacity should be determined by considering the cost and the fleet operation. Fig. 6 shows that the fleet size increases when the wait time constraint decreases and the target reliability increases, whereas the battery capacity does not show such a tendency. Therefore, the battery capacity is determined considering the tradeoff between the battery capacity and the fleet size to reduce the cost while satisfying the target reliability of the customer wait time, which is influenced by the fleet size, range, and CS wait time.

4) *RBDO does not minimize the CS wait time, but designs the CS considering the customer wait time and the CS cost so that the CS wait time does not deteriorate the reliability of the customer wait time*. The mean CS wait time determined from the designs of the SAEV system are presented in Table 10. Each mean CS wait time is affected by the fleet size and the battery capacity but is also related to the number of CSs and the number of chargers in each CS, which are associated with the capacity of the CSs. The decision variables in the SAEV system directly affect the customer wait time, but also indirectly affect the customer wait time through the CS wait time. As in the queuing theory, reducing the CS wait time is advantageous to the operation; however, the CS is designed by considering the influence of the CS wait time on the customer wait time and the appropriate CS wait time is determined as the CS design is related to cost. When the target reliability increases, increasing the number of CSs and the number of chargers in each CS to reduce the CS wait time can result in a significant increase in the charging station cost; therefore, the CS cost and the relationships between the factors affecting the customer wait time are considered in RBDO to satisfy the target reliability while minimizing the cost.

Table 10 Mean CS wait time

Wait time constraint (min)	DO design	RBDO design	
		P_F^{Target}=10%	P_F^{Target}=5%
6	29.4 min	24.4 min	22.4 min
8	26.5 min	50.9 min	19.0 min
10	33.0 min	33.0 min	24.3 min
12	23.0 min	33.9 min	16.6 min

5) *RBDO can reduce the customer's inconvenience by reducing the customer wait time in rush hour*

compared with DO. To investigate the characteristic and tendency of the customer wait time under different wait time constraints and target reliabilities, the mean customer wait time vs. time graphs for 24 h are presented in Fig. 7. Owing to the increase in traffic and trip requests during rush hour, the customer wait time tends to increase during rush hour: it increases 44.88% (4.47 min) in the DO design; it increases 37.81% (2.12 min) in the RBDO design with 90% reliability; and it increases 36.95% (1.72 min) in the RBDO design with 95% reliability. In the RBDO design, the overall customer wait time is smaller than that of the DO design, and the increase in customer wait time during rush hour in particular is decreased compared with that in the DO design. Therefore, in the SAEV system designed using DO, the customer wait time increases significantly during rush hour when customers have to take the SAEV quickly, causing serious inconvenience. Moreover, when the target reliability is increased in the RBDO design, the customer wait time during rush hour is further decreased to satisfy the given target reliability. As the target reliability of the RBDO design increases and the wait time constraint decreases, the SAEV system is designed to reduce the increase in customer wait time during rush hour, thereby satisfying the target reliability of the customer wait time.

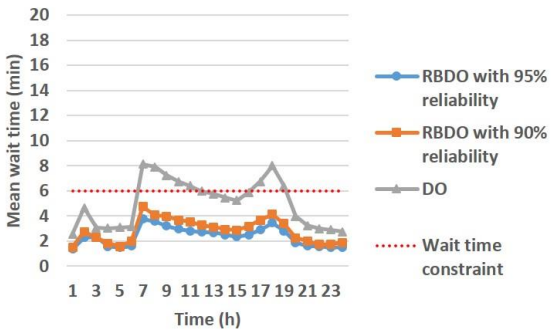

(a) Wait time constraint of 6 min

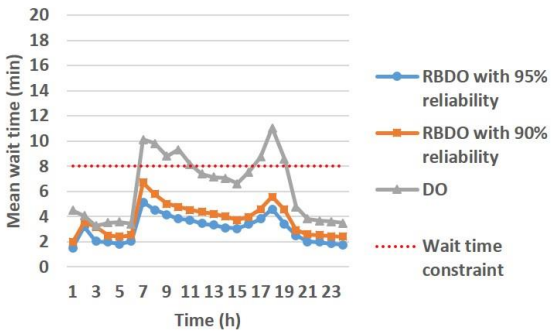

(b) Wait time constraint of 8 min

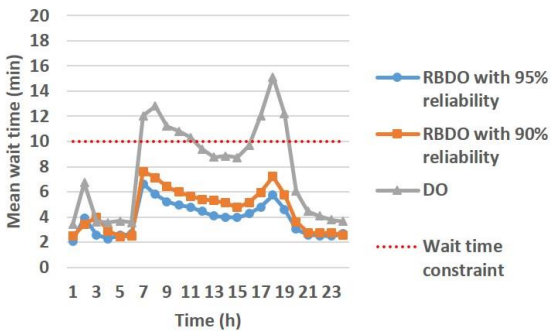

(c) Wait time constraint of 10 min

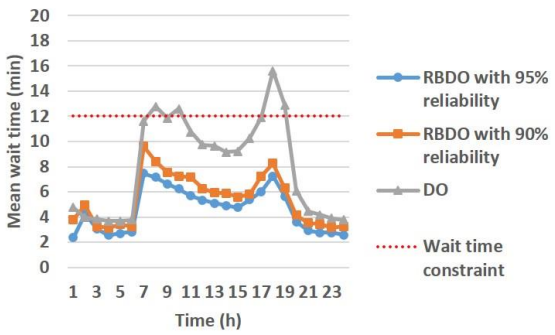

(d) Wait time constraint of 12 min

Fig. 7 Mean customer wait time vs. time graphs for 24 h

6) *RBDO design can achieve robustness of the customer wait time.* Fig. 8 shows the distribution of customer wait time according to the wait time constraint. The DO design can cause inconvenience to customers owing to the high possibility of having excessive customer wait time. Furthermore, a large variation in the customer wait time makes it difficult to predict it. However, the variance of the distribution of the customer wait time decreases when RBDO is applied, and the variance further decreases as the target reliability increases. Therefore, the RBDO design can secure the target reliability and achieve robustness of the customer wait time simultaneously.

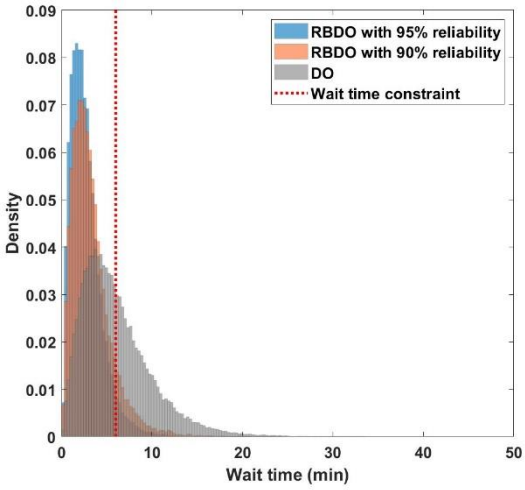

(a) Wait time constraint of 6 min

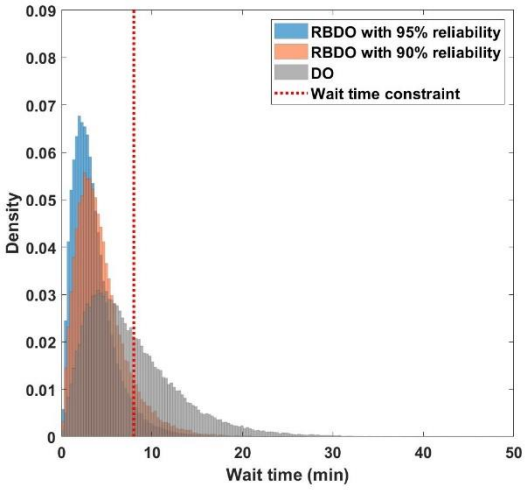

(b) Wait time constraint of 8 min

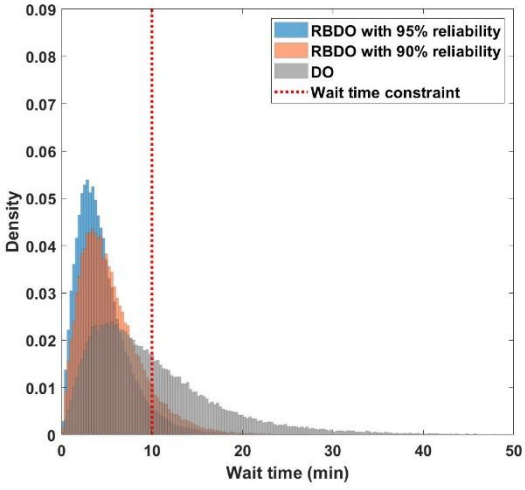

(c) Wait time constraint of 10 min

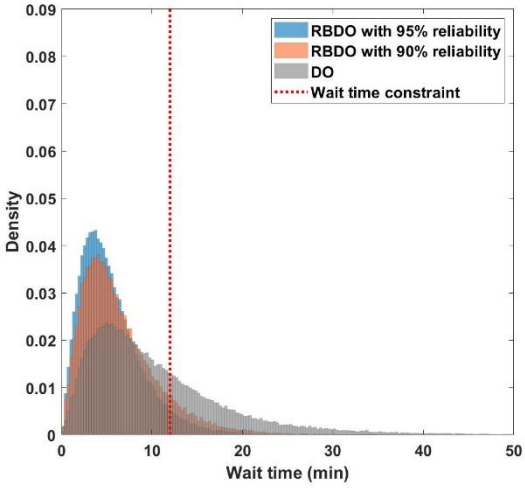

(d) Wait time constraint of 12 min

Fig. 8 Distribution of customer wait time

4.3 Sensitivity analysis and parametric studies

To determine the effect of uncertainties in the SAEV system on the customer wait time, a global sensitivity analysis is performed by using Sobol's method, and the result is presented in Table 11. Under a probabilistic system in which uncertainties are considered, Sobol's method decomposes the variance of the output of the system into fractions affected by the inputs. The Sobol index indicates how much the input affects the output variance. As the Sobol index of the traffic is the largest, the traffic has a large effect on the customer wait time; therefore, accumulating traffic data through an accurate traffic survey of each road section is important for applying RBDO to the design of the SAEV system. Furthermore, uncertainties related to trip requests have a considerable effect on the customer wait time, and rigorous investigation on the trip requests over time is necessary.

Table 11 Sobol index of uncertainties

	Cell weight	Cell capacity	Cell voltage	Initial SOC	Origin & destination	Request time	Traffic
Sobol index	0.12933	0.12228	0.10158	0.12208	0.15535	0.16398	0.86415

Various parametric studies are performed to obtain observations on applying RBDO to the design of the SAEV system with different conditions.

1) *A large error in the probability of failure occurs if the real-time traffic is not reflected, but the error tends to decrease as the target reliability of RBDO increases.* To demonstrate the importance of reflecting the real-time traffic of each road section, the results of RBDO obtained without considering real-time traffic are compared with the results of RBDO obtained by considering real-time traffic. Table 12 shows the probability of failure obtained when simulating the optimal design, which is derived without considering the real-time traffic, on an actual system having traffic. The difference between the probability of failure and the target probability of failure becomes small as the target reliability increases. This is because the uncertainty arising from not considering the real-time traffic can be compensated when the target reliability is high, but this effect is reduced when the target reliability is low.

Table 12 Probability of failure of the optimal design derived without considering real-time traffic

Wait time constraint (min)	DO design	RBDO design	
		P_F^{Target}=10%	P_F^{Target}=5%
6	66.366%	33.861%	25.262%
8	64.288%	37.382%	25.024%
10	71.438%	32.242%	26.954%
12	66.938%	30.184%	22.581%

2) *Applying the wait time constraint only to the rush hour increases the total cost, but the increase rate of total cost decreases as the target reliability of RBDO increases.* The optimization is performed by applying the wait time constraint only to the rush hour rather than over the entire 24 h. In both DO and RBDO designs, the total cost increases when the wait time constraint is applied only to the rush hour. This is because the wait time constraint is applied only to the customer wait time during rush hour, which is increased owing to the increased traffic and trip requests; thus, a conservative design that can further reduce the customer wait time is derived. A comparison of the increase rate of the total cost when the wait time constraint is applied only to rush hour is shown in Fig. 9. As the target reliability increases, the increase rate of total cost is lowered as the increase in the customer wait time during rush hour becomes relatively small: it increases 31.29% in the DO design; it increases 26.68% in the RBDO design with 90% reliability; and it increases 23.39% in the RBDO design with 95% reliability.

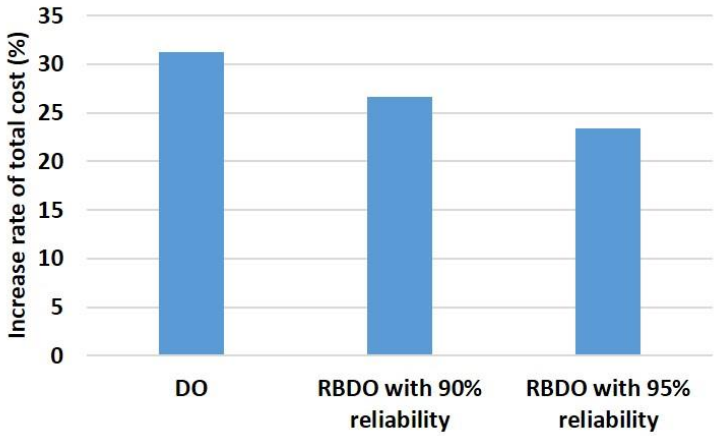

Fig. 9 Increase rate of the total cost when the wait time constraint is applied only to rush hour

3) *RBDO is insensitive to the increase in the number of trip requests compared with DO and becomes more*

insensitive as the target reliability increases. The optimization problem is solved with different numbers of trip requests: i.e., with a 50% decrease and 50% increase in the trip requests from the current number of trip requests. A comparison of the increase rate of the total cost when the number of trip requests changes is shown in Fig. 10. As expected, the total cost increases for both DO and RBDO designs as the number of trip requests increases. However, the increase rate of the total cost of the RBDO design (6.26%) is much smaller than that of the DO design (29.78%), and as the target reliability of the RBDO design increases, the increase rate of the total cost tends to decrease (from 8.54% to 3.98%). As RBDO pursues a conservative design to ensure the target reliability of the customer wait time, the RBDO design is insensitive to the increase in the number of trip requests, and thus, the rate of increase of the total cost is small.

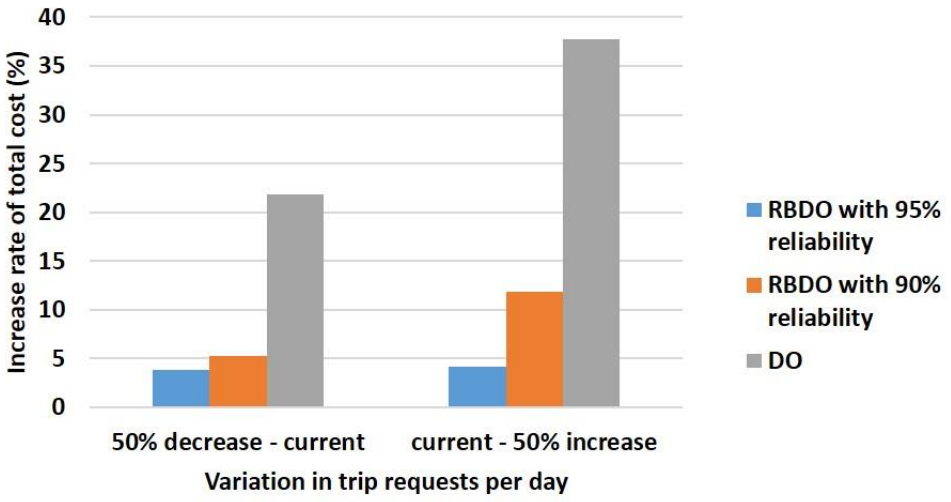

Fig. 10 Increase rate of the total cost when the number of trip requests changes

5. Conclusion

In this study, RBDO is successfully applied to the design of an SAEV system considering the uncertainties in the SAEV system. Real road connections of a city are realized using nodes and segments, and the real-time traffic of each road section is reflected. As the probability of failure of the customer wait time is large when the design of the SAEV system is optimized through DO, deriving the design of the SAEV system that secures the target reliability of the customer wait time by applying RBDO is important. The results of RBDO using various wait time constraints and target reliabilities show how the fleet size, battery design, and CS design interact with

each other and how the optimal values are determined to minimize the cost while satisfying the target reliability.

From the optimal designs and outcomes, the following observations can be made. First, as the target reliability of the RBDO design increases, the total cost increases significantly. Second, in both DO and RBDO designs, the fleet size tends to increase as the wait time constraint decreases, and a CS design where chargers are distributed over a large area is preferred. Third, there is a tradeoff relationship between the battery capacity and the fleet size, and the battery capacity is determined by considering the cost in addition to the range, CS wait time, and fleet size, which affect the fleet operation. Fourth, RBDO does not minimize the CS wait time, but designs CS so that the CS wait time does not deteriorate the reliability of the customer wait time. Fifth, by reducing the customer wait time during rush hour, RBDO reduces the customer's inconvenience. Finally, the RBDO design can achieve robustness of the customer wait time. A global sensitivity analysis for the uncertainties in the SAEV system is performed using Sobol's method. The Sobol index of the traffic is the largest, which indicates that the traffic affects the customer wait time the most.

From various parametric studies, several insights can be obtained. First, if the real-time traffic is not reflected in the design of the SAEV system, a large error in the probability of failure occurs, but the error tends to decrease as the target reliability of RBDO increases. Second, applying the wait time constraint only to the rush hour increases the total cost, but the increase rate of the total cost decreases as the target reliability of RBDO increases. Finally, RBDO is insensitive to the increase in the number of trip requests compared with DO and becomes more insensitive as the target reliability increases.

This study is a novel application of RBDO to the design of an SAEV system and presents a consideration of designs that can satisfy the target reliability of the customer wait time under any uncertainties. A design framework of the SAEV system that can both lower the cost and ensure the reliability of the customer wait time is proposed. There are some limitations to this study. Future studies should focus on determining the next destination of the SAEV when free floating, perform accurate quantification of uncertainties in the SAEV system, and remove some assumptions used in this work. The wait time constraint of the probabilistic constraint and the target reliability can be determined by introducing a design for market systems (Kang et al., 2015, 2018) and a reliability-based design for market systems, respectively (Lee et al., 2019).

6. Acknowledgments

This work was supported by the National Research Foundation of Korea (NRF) grants funded by the Korea government (MSIT) (No. 2017R1C1B2005266 and No. 2018R1A5A7025409) and a grant (17TLRP-C135446-

01, Development of Hybrid Electric Vehicle Conversion Kit for Diesel Delivery Trucks and its Commercialization for Parcel Services) from the Transportation & Logistics Research Program (TLRP) funded by the Ministry of Land, Infrastructure and Transport of the Korean government.

7. Conflict of Interest

On behalf of all authors, the corresponding author states that there is no conflict of interest.

8. Replication of Results

The code for this paper is available at the website:

(https://drive.google.com/drive/folders/1FLk_12YGDJV1pD2-LDwO2giPeNK3VcrO).

References

Bösch, P. M., Becker, F., Becker, H., Axhausen, K. W., 2017. Cost-based analysis of autonomous mobility services. Transp. Policy 59, 1–16.

Chen, T. D., Kockelman, K. M., 2016. Management of a shared, autonomous, electric vehicle fleet: implications of pricing schemes. Transp. Res. Rec. 2572, 37–46.

Chen, T. D., Kockelman, K. M., Hanna, J. P., 2016. Operations of a shared, autonomous, electric vehicle fleet: Implications of vehicle & charging infrastructure decisions. Transp. Res. Part A 94, 243–254.

Chen, Z., He, F., Yin, Y., Du, Y., 2017. Optimal design of autonomous vehicle zones in transportation zones. Transp. Res. Part B, 99, 44–61.

Chiti, H., Khatibinia, M., Akbarpour, A., Naseri, H., 2016. Reliability-based design optimization of concrete gravity dams using subset simulation. Int. J. Optim. Civil Eng. 6(3), 329–348.

Choi, K. K., Youn, B. D., 2002. On Probabilistic Approaches for Reliability-Based Design Optimization. Proceedings of 9th AIAA/ NASA/USAF/ISSMO Symposium on Multidisciplinary Analysis and Optimization, Atlanta, GA, Sept. 4–6.

Daejeon Metropolitan City, 2019. Trade Area Analysis of Daejeon. Daejeon Metropolitan City, accessed June 14, 2019, https://www.daejeon.go.kr/drh/DrhContentsHtmlView.do?menuSeq=5291

Dijkstra, E., 1959. A note on two problems in connexion with graphs. Numer. Math., 1, 269–271.

Dubarry, M., Vuillaume, N., Liaw, B. Y., 2010. Origins and accommodation of cell variations in Li-ion battery pack modeling. Int. J. Energy Res. 34(2), 216–231.

EERE, 2016. Study shows average cost of electric vehicle charger installations. U.S. Department of Energy, https://www.energy.gov/eere/vehicles/fact-910-february-1-2016-study-shows-average-cost-electric-vehicle-charger

Electric Vehicle Charging Information System, 2019. Electric vehicle state. Electric Vehicle Charging Information System, accessed June 26, 2019, https://www.ev.or.kr/eng/Sub1_3.jsp

Energy Saver, 2015. Saving money with electric vehicles. U.S. Department of energy, accessed May 20, 2019, https://www.energy.gov/energysaver/articles/saving-money-electric-vehicles

EV Specifications, 2019. 2019 Nissan Leaf SV Plus. EV Specifications, accessed June 20, 2019, https://www.evspecifications.com/en/model/bbbd9a

Farhan, J., Chen, T. D., 2018. Impact of ridesharing on operational efficiency of shared autonomous electric vehicle fleet. Transp. Res. Part C 93, 310–321.

Fiori, C., Ahn, K., Rakha, H. A., 2016. Power-based electric vehicle energy consumption model: model development and validation. Appl. Energy 168, 257–268.

Frangopol, D. M., Maute, K., 2003. Life-cycle reliability-based optimization of civil and aerospace structures. Comput. Struct. 81(7), 397–410.

Hadigol, M., Maute, K., Doostan, A., 2015. On uncertainty quantification of lithium-ion batteries: application to an LiC6/LiCoO2 cell. J. Power Sources 300, 507–524.

Hyland, M., Mahmassani, H. S., 2018. Dynamic autonomous vehicle fleet operations: optimization-based strategies to assign AVs to immediate traveler demand requests. Transp. Res. Part C 92, 278–297.

Iacobucci, R., McLellan, B., Tezuka, T., 2018. Modeling shared autonomous electric vehicles: potential for transport and power grid integration. Energy 158, 148–163.

Iacobucci, R., McLellan, B., Tezuka, T., 2019. Optimization of shared autonomous electric vehicles operations with charge scheduling and vehicle-to-grid. Transp. Res. Part C 100, 34–52.

Jing, R., Xi, Z., Yang. X. G., Decker, E., 2014. A systematic framework for battery performance estimation considering model and parameter uncertainties. Int. J. Prognost. Health Manage. 5(2), 1–10.

Kang, N., Feinberg, F. M., Papalambros, P. Y., 2015. Integrated Decision Making in Electric Vehicle and Charging Station Location Network Design. J. Mech. Des. 137(6), 061402.

Kang, N., Feinberg, F. M., Papalambros P. Y., 2016a. Autonomous electric vehicle sharing system design. J. Mech. Des. 139(1), 011402.

Kang, N., Ren, Y., Feinberg, F. M., Papalambros, P. Y., 2016b. Public Investment and Electric Vehicle Design: A Model-based Market Analysis Framework With Application to a USA-China Comparison Study. Des. Sci., 2, e6.

Kang, N., Bayrak, A., Papalambros, P. Y., 2018. Robustness and Real Options for Vehicle Design and Investment Decisions under Gas Price and Regulatory Uncertainties. J. Mech. Des. 140(10), 101404.

Korea Ministry of Land, Infrastructure and Transport, 2011. Characteristics of taxi and traffic situation. Korea Ministry of Land, Infrastructure and Transport, http://www.molit.go.kr/USR/NEWS/m_71/dtl.jsp?lcmspage=53&id=95069297

Lee, T., Jung, J., 2008. A sampling technique enhancing accuracy and efficiency of metamodel-based RBDO: constraint boundary sampling. Comput. Struct. 86(13–14), 1463–1476.

Lee, J., Kang, H. Y., Kwon, J. H., Kwak, B. M., 2009. Reliability of aerodynamic analysis using a moment method. Int. J. Comput. Fluid. Dyn. 23(6), 495–502.

Lee, I., Choi, K. K., Gorsich, D., 2010. Sensitivity analysis of FORM-based and DRM-based performance measure approach (PMA) for reliability-based design optimization (RBDO). Int. J. Numer. Methods. Eng. 82(1), 26–46.

Lee, I., Choi, K. K., Zhao, L., 2011. Sampling-based RBDO using the stochastic sensitivity analysis and dynamic Kriging method. Struct. Multidisc. Optim. 44(3), 299–317.

Lee, I., Shin, J., Choi, K. K., 2013. Equivalent target probability of failure to convert high-reliability model to low-reliability model for efficiency of sampling-based RBDO. Struct. Multidiscip. Optim. 48(2), 235–248.

Lee, U., Kang, N., Lee, I., 2019. Selection of optimal target reliability in RBDO through reliability-based design for market systems (RBDMS) and application to electric vehicle design. Struct. Multidisc. Optim. 1–15.

Liang, X., Correia, G. H. D. A., van Arem, B., 2016. Optimizing the service area and trip selection of an electric automated taxi system used for the last mile of train trips. Transp. Res. Part E: Logist. Transp. Rev. 93, 115–129.

Lim, J., Lee, B., Lee, I., 2015. Post optimization for accurate and efficient reliability-based design optimization using second-order reliability method based on importance sampling and its stochastic sensitivity analysis. Int. J. Numer. Method. Eng. 107(2), 93–108.

Litman, T., 2014. Autonomous vehicle implementation predictions. Vic. Transp. Policy Inst., 28.

Loeb, B., Kockelman, K. M., Liu, J., 2018. Shared autonomous electric vehicle (SAEV) operations across the Austin, Texas network with charging infrastructure decisions. Transp. Res. Part C 89, 222–233.

Luo, Y., Li, A., Kang, Z., 2011. Reliability-based design optimization of adhesive bonded steel-concrete composite beams with probabilistic and non-probabilistic uncertainties. Eng. Struct. 33(7), 2110–2119.

Mak, H. Y., Rong, Y., Shen, Z. J. M., 2013. Infrastructure planning for electric vehicles with battery swapping. Manage. Sci. 59(7), 1557–1575.

Marwaha, G., Kokkolaras, M., 2015. System-of-systems approach to air transportation design using nested optimization and direct search. Struct. Multidisc. Optim. 51(4), 885–901.

Meyer, J., Becker, H., Bösch, P. M., Axhausen, K. W., 2017. Autonomous vehicles: the next jump in accessibilities?. Res. Transp. Econ. 62, 80–91.

Miao, H., Jia, H., Li, J., Qiu, T. Z., 2019. Autonomous connected electric vehicle (ACEV)-based car-sharing system modeling and optimal planning: A unified two-stage multi-objective optimization methodology. Energy 169, 797–818.

Missoum, S., Dribusch, C., Beran, P., 2010. Reliability-based design optimization of nonlinear aeroelasticity problems. J. Aircr. 47(3), 992–998.

NAVER map, 2019. NAVER map. NAVER map, accessed July 13, 2018, https://map.naver.com/

Nguyen, V. S., Jeong, M. C., Han, T. S., Kong, J. S., 2013. Reliability-based optimisation design of post-tensioned concrete box girder bridges considering pitting corrosion attack. Struct. Infrastruct. Eng. 9(1), 78–96.

Noh, Y., Choi, K. K., Lee, I., 2009. Reduction of ordering effect in reliability-based design optimization using dimension reduction method. AIAA J. 47(4), 994–1004.

Qu, X., Venkataraman, S., Haftka, R. T., Johnson, T. F., 2003. Deterministic and reliability based optimization of composite laminates for cryogenic environments. AIAA J. 41(10), 2029–2036.

Shin, J., Lee, I., 2014. Reliability-based vehicle safety assessment and design optimization of roadway radius and speed limit in windy environments. J. Mech. Des. 8(136), 081006.

Shin, J., Lee, I., 2015. Reliability analysis and reliability-based design optimization of roadway horizontal curves using a first-order reliability method. Eng. Optim. 47(5), 622–641.

Simpson, A., 2006. Cost-benefit analysis of plug-in hybrid electric vehicle technology. 22nd International Battery, Hybrid and Fuel Cell Electric Vehicle Symposium and Exhibition, National Renewable Energy Laboratory, Yokohama, Japan, Oct. 23–28, Paper No. NREL/CP-540-40485.

Tansel, B. C., Francis, R. L., Lowe, T. J., 1983. State of the art-location on networks: a survey—part i: the p-center and p-median problems. Manage. Sci. 29(4), 482–497.

The Mack Institute, 2017. Analysis shows continued industry-wide decline in electric vehicle battery costs. The Mack Institute, https://mackinstitute.wharton.upenn.edu/2018/electric-vehicle-battery-costs-decline/

Thompson, M. D., Eamon, C. D., Rais-Rohani, M., 2006. Reliability-based optimization of fiber-reinforced polymer composite bridge deck panels. J. Struct. Eng. 132, 1898–1906.

Tong, W., Koh, W. Q., Birgersson, E., Mujumdar, A. S., Yap, C, 2015. Correlating uncertainties of a lithium-ion battery: a Monte Carlo simulation. Int. J. Energy. Res. 39(6), 778–788.

Tu, W., Li, Q., Fang, Z., Shaw, S., Zhou, B., Chang, X., 2016. Optimizing the locations of electric taxi charging stations: a spatial–temporal demand coverage approach. Transp. Res. Part C 65, 172–189.

Youn, B. D., Choi, K. K., Yang, R. J., Gu, L., 2004. Reliability-based design optimization for crashworthiness of vehicle side impact. Struct. Multidisc. Optim. 26(3–4), 272–283.

Youn, B. D., Choi, K. K., Tang, J., 2005. Structural durability design optimization and its reliability assessment. Int. J. Prod. Dev. 1(3/4), 383–401.

Zhao, L., Choi, K. K., Lee, I., Gorsich, D., 2013. Conservative surrogate model using weighted Kriging variance for sampling-based RBDO. J. Mech. Des. 135(9), Article 091003.

Zhou, X., Walker, P., Zhang, N., Zhu, B., 2013. Performance improvement of a two speed EV through combined gear ratio and shift schedule optimization. SAE Technical Paper 2013-01-1477.

Zou, T., Mahadevan, S., 2006. A direct decoupling approach for efficient reliability-based design optimization. Struct. Multidisc. Optim. 31(3), 190–200.